Engineering Solid Mechanics 7 (2019) 47-58

Contents lists available at GrowingScience

Engineering Solid Mechanics

homepage: www.GrowingScience.com/esm

Mathematical modeling of mass spring's system: Hybrid speed bumps application for mechanical energy harvesting

Chouaib Ennawaoui[a,b*], Houda Lifi[a,c], Abdelowahed Hajjaji[a], Abdessamad Elballouti[a], Said Laasri[a] and Az-eddine Azim[a,b]

[a]*Laboratory of Engineering Sciences for Energy, National School of Applied Sciences El Jadida, UCD, 24000 El Jadida, Morocco*
[b]*Laboratory of Mechanics and Energy, Faculty of Sciences El Jadida, UCD, 24000 El Jadida, Morocco*
[c]*Laboratory of Physics and Nuclear, Atomic and Molecular Techniques, Faculty of Sciences El Jadida, UCD, 24000 El Jadida, Morocco*

A R T I C L E I N F O

Article history:
Received 10 September, 2018
Accepted 5 November 2018
Available online
5 November 2018

Keywords:
Energy harvesting
Mass-spring
Hybrid system
Mechanical system
Piezoelectric polymers

A B S T R A C T

The aim of this paper is to provide a theoretical analysis on the mechanical power of the mass spring's system. Some tests are conducted to experimentally evaluate the theoretical analysis and to investigate the mechanical energy ability of this concept. The authors suggest a system used for applications of energy harvesting from roads. The system is able to transform the kinetic energy produced by the passage of vehicles on the road for electrical energy based on the mass-spring using two technologies. The hybrid system has two goals. First, supply the entourage by a mechanism to produce significant electrical power used mainly for public lighting. A device is also provided for storing electrical energy for later use, for home lighting at night or in the case of bad weather. Second, the piezoelectric subsystem controls the spring's health through analyzing the amplitude and shape of the voltage generated by a piezoelectric material. Finally, an experimental validation of the designed smart speed bump is presented.

© 2019 Growing Science Ltd. All rights reserved.

1. Introduction

Over the past decade, many electrically powered systems have emerged from ambient vibrations. Interest in ambient energy harvesting (El Fatnani et al., 2016a) is intimately linked to the ability to measure, monitor, process, a sometimes hostile environment and to be able to communicate them completely independently (El Fatnani et al., 2016 b; Lifi et al., 2017). When a very large number of sensors are dispersed in an environment, it is necessary that they are provided with a power supply of the longest possible life to limit maintenance, which is also impossible under certain conditions. The most commonly adopted solution is to draw from the source of mechanical energy, a priori infinite, induced by the vibrations of the immediate environment of the sensor (Nassit & Berbia 2015; Sborikas et al., 2016; Jandaghian et al., 2014). The conversion of the mechanical energy into electrical energy (Manbachi & Cobbold 2011; Ennawaoui et al., 2018 a) is carried out by an electromechanical generator. Several technologies (Talebi et al., 2015; Wang et al., 2015) exist but the most "conventional", allowing converting the energy of the surrounding vibrations, exploiting electromagnetic conversions (Le et al., 2014; Pirisi et al., 2013; Belouadah, 2017; Pirisi et al., 2009), piezoelectric (Ennawaoui et al., 2016;

* Corresponding author. Tel. : +212 5 23 39 56 79 Fax: +212 5 23 39 49 15
E-mail addresses: chouaib.enna@gmail.com (C. Ennawaoui)

© 2019 Growing Science Ltd. All rights reserved.
doi: 10.5267/j.esm.2018.11.002

Wang et al., 2018; Eddiai et al., 2013; Kaewkongka 2016) or mechanisms. The last focuses on electromechanical systems exploiting the piezoelectric effect or of the conversion by a mechanism.

This paper is organized as follows. Section 2 provides the theoretical model on the mechanical power of a generic system mass springs. Then, the tests are conducted to experimentally evaluate the theoretical model and a comparison between the theoretical and the experimental results in Section 3. Section 4 introduces the design of the proposed roadway harvesting system and the composition of each subsystem. Sections 5 investigate the energy harvesting capability of the mechanical subsystem and the piezoelectric subsystem. Finally, conclusions from this study are drawn in Sec. 6.

This work proposes a novel hybrid energy-regenerative system which integrates the combined piezoelectric materials and mechanisms based on the mass spring's system.

2. Theoretical modeling of the mechanical power generated by the mass spring's system

Springs are now widely used in all kinds of machines and equipment. Their functions are very diverse. One can quote, without precise order: recall of a part removed from its equilibrium position, maintenance of a clamping force (clothespins), fast opening (knife with stop, hand-left trident), suspension of a vehicle (leaf springs, helical springs, Hydropneumatic systems), motor spring and shock absorbers (railway material pads),

It is very often useful to know the stiffness *K* of a coil spring. For this we use the Eq. (1):

$$K = \frac{Ed^4}{16(1+\vartheta)nD^3}, \tag{1}$$

where *K* is the spring stiffness, *E* is the Young's modulus, ϑ is the Poisson's coefficient, dimensionless, equal to 0.33 for steels, *n* is the number of useful turns (without unit), *d* is the diameter of the wire and *D* is the average diameter or winding diameter of the turns (the average between the inside and outside diameters of the turns). The goal of modeling the system is to quantify the mechanical energy and displacement generated during the application of a compression stress. Inertial-based generators are essentially second-order, spring-mass systems. Fig. 1 shows a general example of such a system based on a seismic mass, M_R, on a spring of stiffness, K_I.

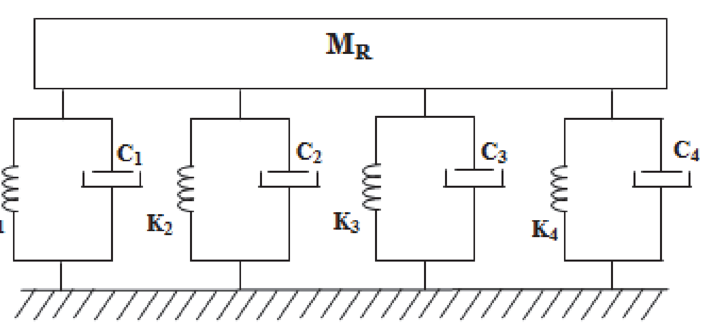

Fig. 1. Schema of the spring's system

It is assumed that the springs having identical stiffness, i.e.

$$K_T = \sum_{i=1}^{4} K_i \,. \tag{2}$$

The moving mass position with respect to the base is marked by the coordinate $x \in R^+$, equal to x_0 when the system is at rest. The mass M_R is connected to the base *S* by a spring *R*, of stiffness $K > 0$. The viscous friction and the loss of mechanical energy are modeled by a shock absorber C_T.

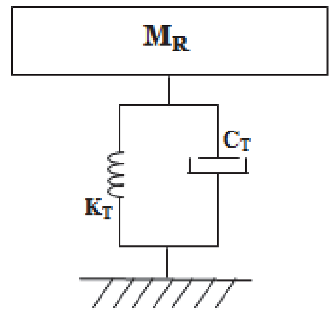

Fig. 2. Equivalent System Scheme

The single degree of liberty helps to study the unidirectional response of the system. The governing equation of motion for the system can be obtained from Alembert's principle applies to a lumped spring mass (Eq. (3)):

$$M_R \frac{d^2 X_S}{dt^2} + C_T \frac{dX_S}{dt} + K_T X_S = C_T \frac{dX_V}{dt} + K_T X_V . \tag{3}$$

Assuming that the mass of the vibration source is significantly greater than that of the seismic mass and therefore not affected by its presence, and also that the external excitation is harmonic. The Laplace transform of a time-dependent function is given by the Eq. (4):

$$\frac{X_S(p)}{X_V(p)} = l\left\{\frac{X_S(t)}{X_V(t)}\right\} = \int_0^{\infty} e^{-pt} \frac{X_S(t)}{X_V(t)} dt . \tag{4}$$

The application of Laplace transform on the Eq. (1) yields,

$$\frac{X_S(p)}{X_V(p)} = \frac{pC_T + K_T}{p^2 M_R + pC_T + K_T} . \tag{5}$$

Then the expression of the displacement is written as follows,

$$S(p) = \frac{1}{M_R} \frac{(pC_T + K_T)}{(p+a)(p+b)} , \tag{6}$$

With a and b the roots of the Eq. (7),

$$p^2 + p\frac{C_T}{M_R} + \frac{K_T}{M_R} = 0 \text{ and } S(p) = \frac{X_S(p)}{X_V(p)} . \tag{7}$$

After solving the equation, the expression of the displacement (Eq. (8)):

$$S(p) = \frac{C_T}{M_R} \frac{\left(p + \frac{K_T}{C_T}\right)}{\left(p + \frac{C_T - \sqrt{C_T^2 - 4K_T M_R}}{2C_T}\right) * \left(p + \frac{C_T + \sqrt{C_T^2 - 4K_T M_R}}{2C_T}\right)} . \tag{8}$$

The standard steady-state solution for the mass displacement is given by the Eq. (9):

$$S(t) = \frac{C_T}{M_R}\left[K e^{-at} + (1-K) e^{-bt}\right] \tag{9}$$

With

$$a = \frac{C_T - \sqrt{C_T^2 - 4K_T M_R}}{2C_T} \quad b = \frac{C_T + \sqrt{C_T^2 - 4K_T M_R}}{2C_T} \quad \text{and} \quad K = \frac{\frac{K_T}{C_T} - a}{b - a}. \tag{10}$$

The speed as a function of time:

$$\frac{dS(t)}{dt} = -\frac{C_T}{M_R}\left[aKe^{-at} + b(1-K)e^{-bt}\right]. \tag{11}$$

The time-dependent effective behavior of mechanical power is obtained by a numerically inverting Eq. (11) to the time domain. The power generated during the stress application:

$$P(t) = F(t)\frac{dS(t)}{dt}, \tag{12}$$

With P (t) the power generated, F (t) the excitation force and R '(t) the linear velocity of the system. The input of the system is excited by a request of the Eq. (13):

$$F(t) = W(t)X, \tag{13}$$

where X: [0, + ∞ [→ R is the function which gives the amplitude of the excitation force (in Newton), this type of excitation is called finite excitation.

$$W(t) = \begin{cases} 1 & \text{The passage of a vehicle happens} \\ 0 & \text{Otherwise} \end{cases} \tag{14}$$

The simplified expression of mechanical power generated is given by the Eq (15):

$$P(t) = W(t)\frac{C_T}{M_R}X\left[-aKe^{-at} - b(1-K)e^{-bt}\right]. \tag{15}$$

The model allows the prediction of the effective behavior of mechanical power in the quasi-static domain while taking into account the spring parameters and other characteristics of the system. Application vibration parameters should be carefully studied before designing the system in order to correctly identify the parameters of operation given the design constraints on system size and maximum permissible X(t). The spring characteristics as shown in Table 1.

Table 1. Characteristics of the springs

Spring properties	Value
Spring stiffness K (N/m)	72
Spring high L (m)	0.3
Average diameter D (m)	0.143
Number of useful turns n (SI)	7

To analyze the motion of springs, images are captured during the mechanical simulation using software for modeling and simulation, based on our model. Fig. 3 shows the evolution of the mechanical power generated by the spring's system as a function of time. The results of these simulations show that it is possible to use compression springs to absorb the excitation stress shown by the response of the system (Fig. 3). These simulations found that the distributed absorbers should be designed such that absorbs a big range of excitation stress. The theoretical model is presented for the sake of comparison with the experimental results obtained with the spring's mass prototype.

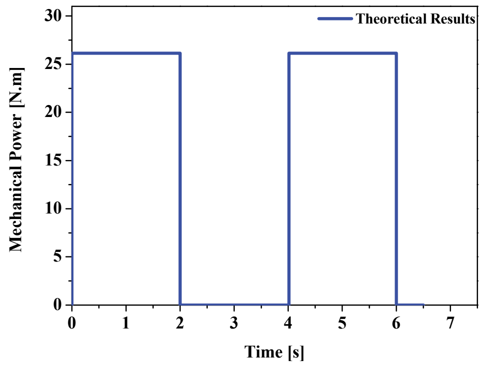

Fig. 3. Theoretical results of mechanical power generated by spring's system

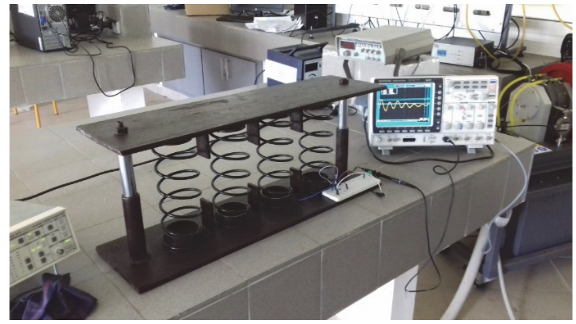

Fig. 4. Complete experiment configuration for spring's system prototype

3. Mass springs prototype and results

The prototype of mass springs system has been manufactured to verify the prediction model, design, analysis, and resulting performance. It is composed of a normalized speed bump, 4 iron springs, 2 Hub shafts for mechanical guidance and a support. In order to achieve the best measuring conditions, a weight has been chosen as an actuator for a generator test bed (Fig. 4). However, the applied forces are measured by a force sensor installed on the system. In particular, we aimed to prove the correspondence between the measurement results and prediction model.

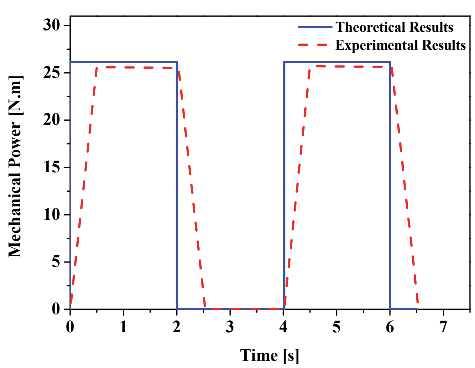

Fig. 5. Theoretical predictions and experimental results on mechanical power generated as a function of time

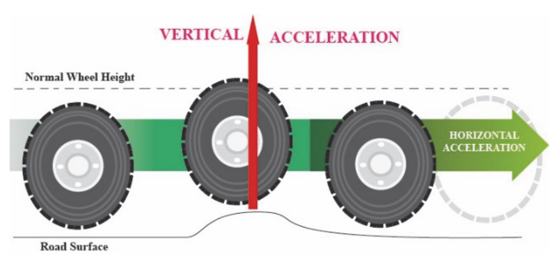

Fig. 6. Problem in a classic speed bump

In Fig. 5, the results of measurements are compared with the simulation expected values. The experimental test results have proven the effectiveness of the model. The results of experimental tests show a good correlation with those of the theoretical model. Both of the curves plotted in Fig. 5 have similar maximum value, which confirms the validity of our model.

4. Application of mass spring's system: Hybrid speed bump

4.1 Global description of the system

The objective of modeling is the system that quantifies the mechanical power absorbed by the mass-springs. The problem caused by the classical speed bump is the energy of the vertically accelerated created by the contact between the vehicle wheel and the speed bump (Fig. 6). So, in order to exploit the mechanical energy generated by the system, it is often necessary to propose a hybrid system coupling piezoelectric materials and a mechanical subsystem is then a promising solution to develop a very compact device able to convert efficiently mechanical energy into electric energy with low frequencies.

The aim of a hybrid system is to transform the mechanical energy produced by the passage of vehicles on it to a usable electrical energy. This innovation has two objectives. First, supply the entourage by a mechanism able to produce significant electrical power, which will be used mainly for public lighting. A device is provided for storing electrical energy for later use, for home lighting at night or in the case of bad weather. Second, the role of the piezoelectric subsystem controls the spring's health through the voltage generated by the piezoelectric material. The advantage of this hybrid system is to convert the kinetic energy produced by the passage of vehicles on the smart speed bump (SSB) to a usable electrical energy. With energy source readily available, "road" energy would be a new energy solution of a renewable energy in terms of the environment, economy, and social needs (Abbasi, 2013; Tanaka & Kawabe, 2016; Sakai, 2008). To provide an effective and time-saving modeling of complex systems, here an appropriate combination of evolutionary techniques can be applied as a convenient means towards SSB global design and performance optimization. The hybrid speed bump was designed using CAD software CATIA V5 2016 (Fig. 7).

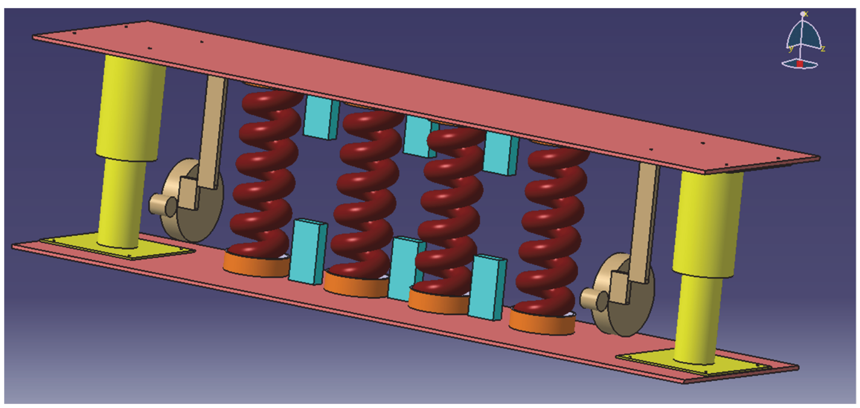

Fig. 7. CAD of Hybrid speed bump system

4.2. Mechanical Subsystem

During the passage of the vehicle on the retarder, the vehicle weight will have the spring to make a translational movement; the connecting crankshaft will convert this movement into a rotational movement. The alternator will convert the rotational motion to an electrical energy (alternative signal). For storage, the use of a rectifier bridge with a battery and necessary.

Therefore, we would like to design this system that can directly replace the traditional speed bump to achieve the desired damping while harvesting the energy. The Fig. 8 and Fig. 9 show the main components and the design of the first subsystem. In the mechanical sub-system, the most important component is the motor (alternator) because it is responsible for electromechanical conversion.

Table 2. Electrical characteristics of the motor

Motor characteristics	Value
Output Power (Watt)	3
Voltage (V)	6

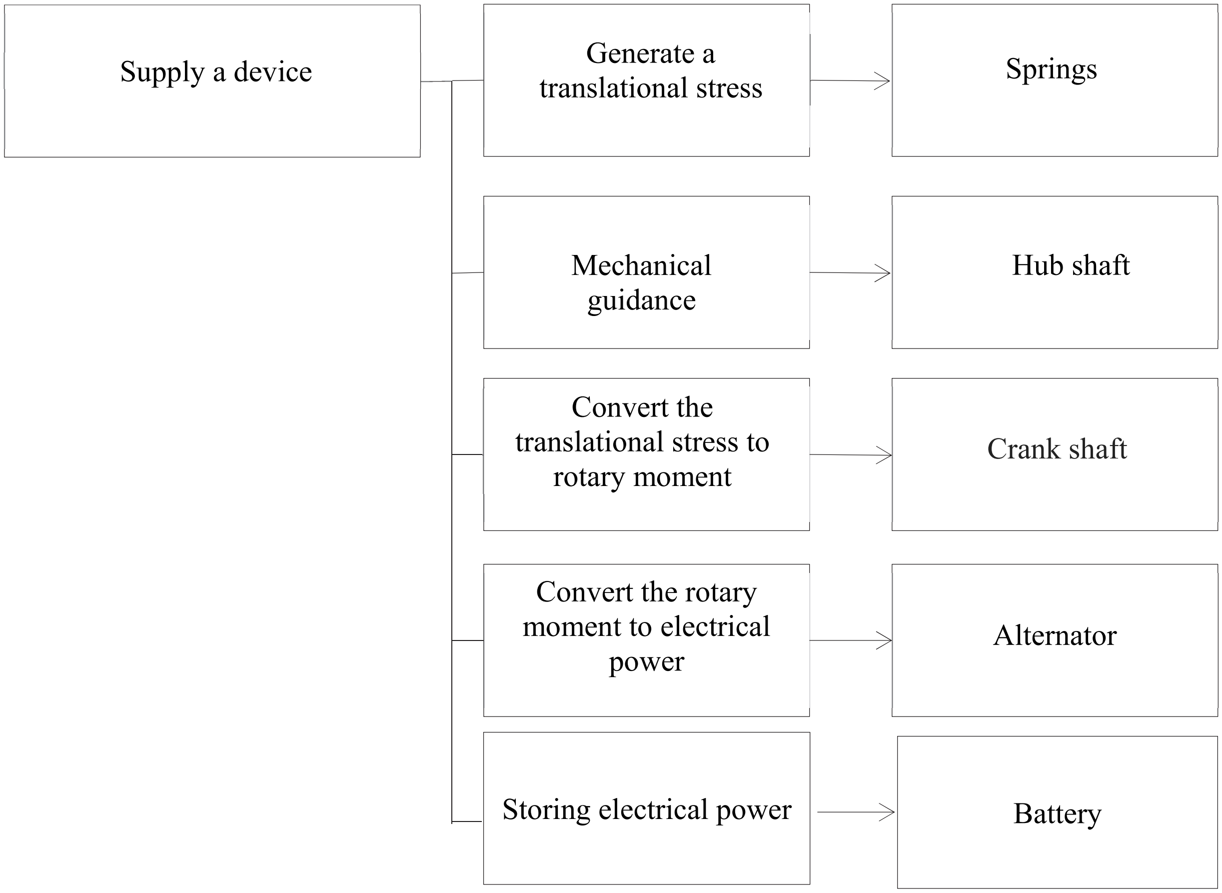

Fig. 8. Mechanical subsystem Functions and Compositions

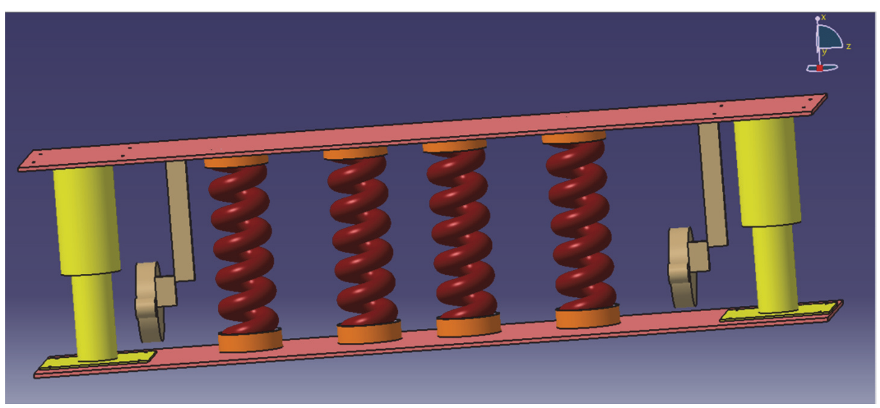

Fig. 9. CAD of mechanical subsystem design

4.3 The Piezoelectric subsystem

Piezoelectric materials provide one approach for converting mechanical to electrical energy and can, therefore, be used to harvest energy from ambient vibration sources. Piezoelectric road integrated technology is a new energy evolution and hence piezoelectric awareness and expertise in this sector is very limited. This was also observed in the literature. Other technical factors were not analyzed in terms of piezoelectric geometry, structure, and thickness in all articles which propose new systems for road energy harvested. Implementing piezoelectric road technology on the field requires a standard specification in the execution process which has not been established. This is important to use appropriate management and method to prevent manipulating with road infrastructure and minimize traffic congestion. The purpose of our second subsystem is to create a current generated by the piezoelectric material to supply a purely resistive load, in our case, it is a sensor. The passage of vehicles on the speed bump will produce mechanical power that is going to be converted into electrical power using PVDF (Rajala & Lekkala, 2012; Chakhchaoui et al., 2017; Rajala & Lekkala, 2010; Ennawaoui et al., 2018b) material and a converter based on an electronic circuit designed to have a current going to be stored in a battery or supply directly a wireless sensor and make it energy independent.

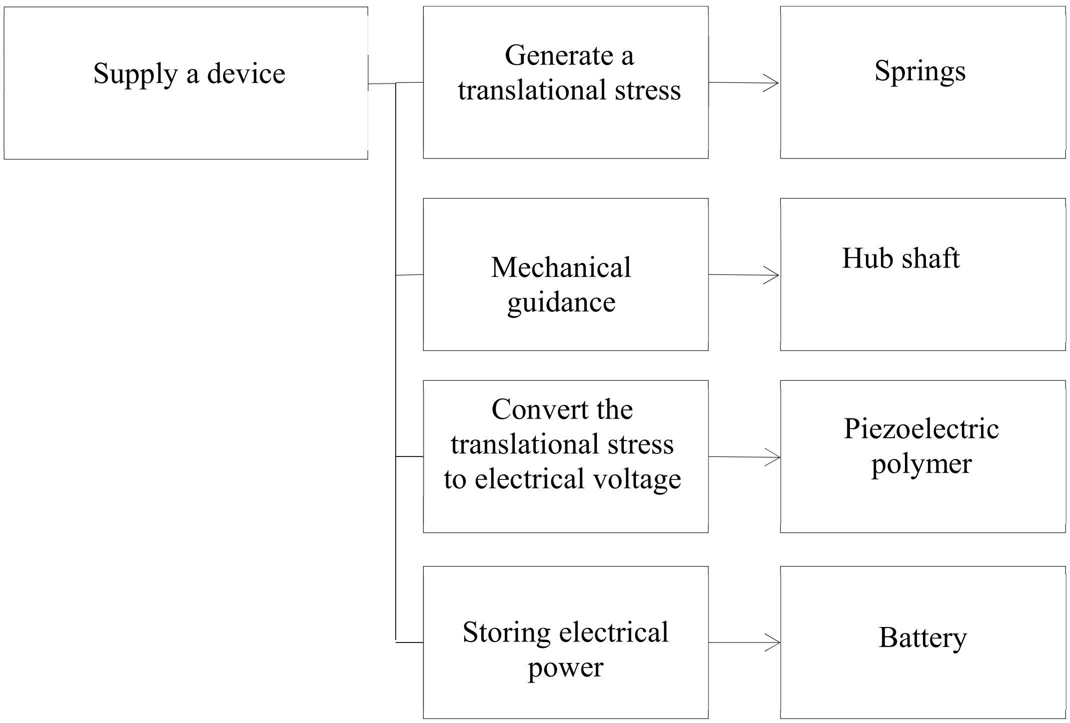

Fig. 10. Piezoelectric subsystem Functions and Compositions

Works have been accomplished on this subject covering either the optimization of the electromechanical structure or development of the techniques of energy i.e. the use of electrical devices to optimize the transfer of energy by impedance matching. The particularity of our approach is to use a transverse vibration mode. The Fig. 10 and Fig. 11 show the main components and the design of the second subsystem.

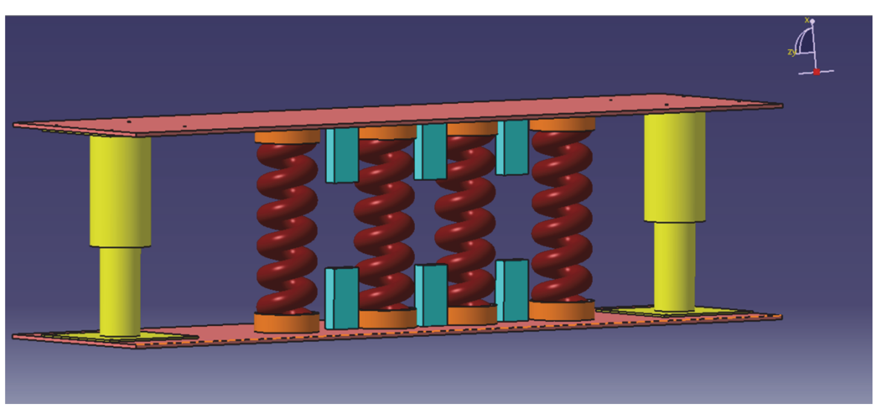

Fig. 11. CAD of Piezoelectric subsystem design

The material used in our work is PVDF. This polymer has the advantage to be flexible and able to deform in the desired geometry. In order to investigate the feasibility of PVDF for road energy harvesting application, the electromechanical proprieties as shown in Table 3.

Table 3. Electromechanical properties of the piezoelectric material

Material properties	Value
Material type	PVDF-110
Coupling factors	12%
Piezoelectric constant d_{33} (pC/N)	33
Capacity C (pF)	113
Young's modulus (N/m²)	2.10^9
Density (10^3 Kg/m³)	1.78
Thickness (µm)	110
Area (mm²)	720

5. Experimental results of energy harvesting system

The energy harvesting system contained the piezoelectric, mechanism and electric circuits. The external circuit was integrated into the system to optimize the harvested voltage output. To obtain the optimum harvesting energy from the hybrid speed bump, the value of external load resistance was chosen as equal to the internal resistors of the material. In this section, the prototype was tested as shown in Fig. 12. The output voltage of the energy harvester system was recorded by the oscilloscope, Gw INSTEK GDS-2074A containing four channels. The hybrid speed bump was manufactured as LabSIPE.

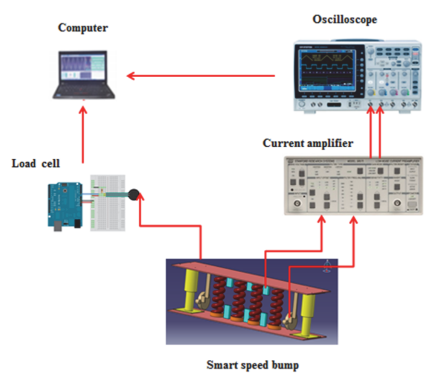

Fig. 12. Experimental setup for the hybrid energy harvesting system.

We tested the performance of the device while it was during the passage of a vehicle (prototype). The average electrical power received by the resistive loads was measured during 8s samples. The device was attached to the oscilloscope, and the average power received by the resistive loads was measured for passage speeds between 30 km/h and 35 km/h (Fig.13).

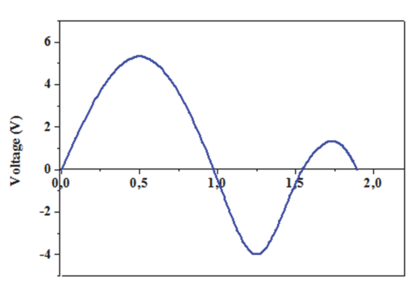

Fig. 13. Voltage Output of mechanical subsystem

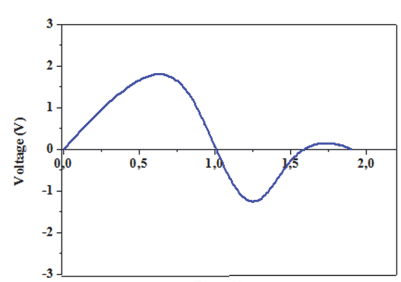

Fig. 14. Voltage Output of piezoelectric subsystem

Fig. 13 and Fig. 14 show the variation of the mechanical subsystem voltage and the piezoelectric subsystem voltage as a function of time for a compression force between 0 and 980 N. During excitation the maximum output voltage reaches a value of the order of 5.6 V for the first subsystem and 2.7 V for the second subsystem. Fig. 15 and Fig. 16 show the evolution of the harvested electrical power at the output as a function of the load resistance during the passage of the vehicles.

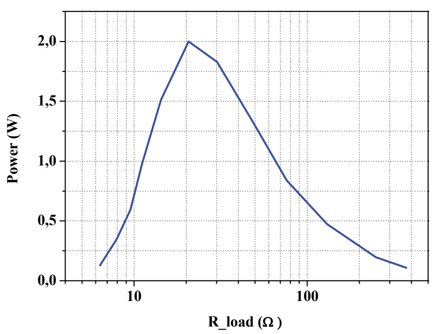

Fig. 15. Power harvested by mechanical subsystem

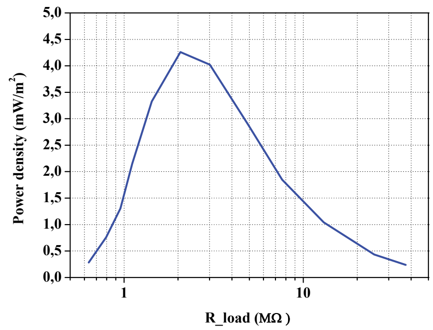

Fig. 16. Power density harvested by piezoelectric subsystem

The load power of the elementary device varies from 1.8 W to 3 W for the first subsystem, while it ranges from 0.5mW to 4.8mW for the second subsystem The form of the electrical voltage in the resistive loads for the device (at 30 km/h) is displayed in Fig. 15 and Fig. 16. The results obtained in this work contribute to demonstrate the ability of the hybrid system between the mechanical and piezoelectric systems to improve the conversion efficiency of the energy produced during the vehicle passage on smart speed bump into electrical energy for the development of l-generators.

Table 4

Comparison between methods

Parameters	Mechanical subsystem	Piezoelectric subsystem
Power harvested	High	Low
Economic	Expensive	Cheap
Implementation	Difficult	Easy
Rentability	Low	High

A comparison between the parameters is needed for the final result. Table 4 gives an overview of the balance between the two methods. The mechanical subsystem is focused mainly on the efficiency, the piezoelectric is on the opposite side more focus on economic and implementation. Since this work is mainly focused on the efficiency of the system, the most interesting system to simulate is the mechanical subsystem. This comparison shows the potential of mass springs system for use in power harvesting applications and provides a means of choosing the piezoelectric device to be used and estimating the amount of time required for it to recharge a specific capacity battery.

6. Conclusion

This paper has presented a new method of enhancing mechanical energy conversion with pulsed mechanical energy. The electromechanical properties and energy harvesting capacities of the hybrid SSB are of great importance from both the points of view of technological interest and fundamental understanding. The present paper has dealt with a combination of a piezoelectric polymer and a mechanical system for energy harvesting capability. More precisely, we have investigated the effect of the vehicle passage on a new speed bump. The proposed model was able to predict the mechanical energy generated by a mass spring's system and provide a good description of the experimental results. Therefore, we conclude that the hybridization of piezoelectric materials and mechanical system is of great interest to obtain a good efficiency of the electromechanical conversion for energy harvesting and a new generation of a system able to combine sensor and generator in the same device.

References

Abbasi, A. (2013). Application of piezoelectric materials and piezoelectric network for smart roads. *International Journal of Electrical and Computer Engineering*, *3*(6), 857.

Belouadah, R., Seveyrat, L., Guyomar, D., Guiffard, B., & Belhora, F. (2016). Magnetoelectric coupling in Fe3O4/P (VDF-TrFE) nanocomposites. *Sensors and Actuators A: Physical*, *247*, 298-306.

Chakhchaoui, N., Ennamiri, H., Hajjaji, A., Eddiai, A., Meddad, M., & Boughaleb, Y. (2017). Theoretical modeling of piezoelectric energy harvesting in the system using technical textile as a support. *Polymers for Advanced Technologies*, *28*(9), 1170-1178.

Eddiai, A., Meddad, M., Sbiaai, K., Boughaleb, Y., Hajjaji, A., & Guyomar, D. (2013). A new technique for maximizing the energy harvested using electrostrictive polymer composite. *Optical Materials*, *36*(1), 13-17.

El Fatnani, F. Z, Guyomar, D., Belhora, F., Mazroui, M. H., Boughaleb, Y., & Hajjaji, A. (2016a). A new concept to harvest thermal energy using pyroeletric effect and Rayleigh-Benard convections. *The European Physical Journal Plus*, *131*(8), 252.

El Fatnani, F. Z., Guyomar, D., Mazroui, M. H., Belhora, F., & Boughaleb, Y. (2016b). Optimization and improvement of thermal energy harvesting by using pyroelectric materials. *Optical Materials*, *56*, 22-26.

Ennawaoui, C., Hajjaji, A., Azim, A., & Boughaleb, Y. (2016). Theoretical modeling of power harvested by piezo-cellular polymers. *Molecular Crystals and Liquid Crystals*, *628*(1), 49-54.

Ennawaoui, C., Lifi, H., Hajjaji, A., Azim, A. E., Elballouti, A., & Rguiti, M. (2018 b). New System to Harvest Road Energy Using Piezoelectric Polymers. *Sensor Letters*, 16(1), 41-47.

Ennawaoui, C., Lifi, H., Hajjaji, A., Laasri, S., Belhora, F., & Azim, A. (2018 a). Piezo-Cellular Polymers for Energy Harvesting in Longitudinal and Transverse Vibration Modes. *Journal of Advanced Physics*, 7(1), 26-32.

Jandaghian, A., Jafari, A., & Rahmani, O. (2014). Vibrational response of functionally graded circular plate integrated with piezoelectric layers: An exact solution. Engineering Solid Mechanics, 2(2), 119-130.

Kaewkongka, T. (2016). Leak detection and localization using acoustic emission technique. Engineering Solid Mechanics, 4(1), 17-24.

Le, M. Q., Belhora, F., Cornogolub, A., Cottinet, P. J., Lebrun, L., & Hajjaji, A. (2014). Enhanced magnetoelectric effect for flexible current sensor applications. *Journal of Applied Physics*, *115*(19), 194103.

Lifi, H., Ennawaoui, C., Hajjaji, A., Touhtouh, S., Benjelloun, M., & Azim, A. (2017). Elaboration, Characterization and Thermal Shock Sensor Application of Pyroelectric Ceramics PMN–xPT. *Sensor Letters*, 15(9), 751-757.

Manbachi, A., & Cobbold, R. S. (2011). Development and application of piezoelectric materials for ultrasound generation and detection. *Ultrasound*, *19*(4), 187-196.

Nassit, M., & Berbia, H. (2015, November). Non-invasive technologies of fetal heart rate diagnosis. In *Complex Systems (WCCS), 2015 Third World Conference on* (pp. 1-5). IEEE.

Pirisi, A., Gruosso, G., & Zich, R. E. (2009, March). Novel modeling design of three phase tubular permanent magnet linear generator for marine applications. In *Power Engineering, Energy and Electrical Drives, 2009. POWERENG'09. International Conference on* (pp. 78-83). IEEE.

Pirisi, A., Mussetta, M., Grimaccia, F., & Zich, R. E. (2013). Novel speed-bump design and optimization for energy harvesting from traffic. *IEEE Transactions on Intelligent Transportation Systems*, *14*(4), 1983-1991.

Rajala, S., & Lekkala, J. (2010). PVDF and EMFi sensor materials—A comparative study. *Procedia Engineering*, *5*, 862-865.

Rajala, S., & Lekkala, J. (2012). Film-type sensor materials PVDF and EMFi in measurement of cardiorespiratory signals—A review. *IEEE Sensors Journal*, *12*(3), 439-446.

Sakai, Y. (2008). Innovation on Energy Power Technology (13) Development of Geothermal Power Generating Facilities. *IEEJ Transactions on Power and Energy*, 128, 1427-1430.

Sborikas, M., Ealo, J. L., & Wegener, M. (2016). Effects of temperature on electromechanical properties and ultrasonic performance of piezoelectric cellular PP films. *Sensors and Actuators A: Physical*, 245, 1-9.

Talebi, N., Sadrnia, M. A., & Darabi, A. (2015). Fault detection of wind energy conversion systems using recurrent neural networks. *International Journal of Sustainable Energy*, *34*(1), 52-70.

Tanaka, K., & Kawabe, K. (2016). Critical Generation Evaluation Using Hybrid Energy Function Method. *Electrical Engineering in Japan*, 196(4), 11-20.

Wang, J., Shi, Z., Xiang, H., & Song, G. (2015). Modeling on energy harvesting from a railway system using piezoelectric transducers. *Smart Materials and Structures*, 24(10), 105017.

Wang, J., Qin, L., Wei, P., & Tang, L. (2018). Modeling and analysis of multilayer piezoelectric-elastic spherical transducers. *Journal of Intelligent Material Systems and Structures*, 1045389X18770868.

© 2018 by the authors; licensee Growing Science, Canada. This is an open access article distributed under the terms and conditions of the Creative Commons Attribution (CC-BY) license (http://creativecommons.org/licenses/by/4.0/).